ELSEVIER

Biophysical Chemistry 100 (2003) 351–366

Biophysical Chemistry

www.elsevier.com/locate/bpc

Thermodynamic characterization of the interaction of human cyclophilin 18 with cyclosporin A☆

Jörg Fanghänel, Gunter Fischer*

Max Planck Research Unit for Enzymology of Protein Folding, Weinbergweg 22, D-06120 Halle (Saale), Germany

Received 12 February 2002; accepted 3 May 2002

Abstract

Isothermal titration calorimetry (ITC) was used to investigate thermodynamic parameters of the cyclosporin A (CsA)-cyclophilin 18 (*h*Cyp18) association reaction. We have calculated the thermodynamic parameters (enthalpy, entropy, heat capacity, and free energy of binding) of the CsA/*h*Cyp18 complexation. All but two methods described in the literature underestimate the affinity to *h*Cyp18 of CsA. We found that the association constant ($1.1 \cdot 10^8$ M^{-1} at 10 °C) of CsA to *h*Cyp18 is in close agreement with the reciprocal of the reported inhibitory constant of the peptidylprolyl *cis*/*trans* isomerase activity of *h*Cyp18. Interpretation of the thermodynamic parameters in buffered solution of water, 30% glycerol and D_2O leads to the conclusion that the highly specific binding of CsA to *h*Cyp18 is mainly mediated through hydrogen bonding and to a lesser degree through hydrophobic interaction. Furthermore, the pH dependence of the association constant was determined and analyzed according to a single proton linkage model, resulting in a pK_a value of 5.7 in free *h*Cyp18 and below 4.5 in the CsA complexed form. Titration experiments using different single component buffers possessing different heats of ionization allowed us to estimate that statistically half a proton is transferred upon CsA binding from the binding interface of *h*Cyp18 to the buffer at pH 5.5. No proton transfer was detected at pH 7.5. The thermodynamic results are discussed in relation to the published X-ray and NMR structure of the free and CsA complexed *h*Cyp18.

Keywords: Cyclophilin; PPIase; Isothermal titration calorimetry; Thermodynamics of molecular interactions

1. Introduction

Human cyclophilin 18 (*h*Cyp18) is the prototypic member of the cyclophilin subfamily of peptidyl prolyl *cis*/*trans* isomerases (PPIases, E.C. 5.1.8). The ubiquitous 165 amino acid long cytosolic protein is the major cytosolic receptor of the hydrophobic cyclopeptide cyclosporin A (CsA) and hence implicated in the CsA-mediated immunosupression [1]. According to the current understanding CsA requires the molecular matchmaker function of *h*Cyp18 for exerting down regulation on a distinct set of lymphokine genes involved in T cell replication [2,3] whereas inhibition of the prolyl isomerase activity is responsible for the blockade of the formation of infectious HIV-1

☆ Dedicated to the memory of John T. Edsall.

*Corresponding author. Tel.: +49-345-5522800; +49-345-5511972.

E-mail address: fischer@enzyme-halle.mpg.de (G. Fischer).

0301-4622/03/$ - see front matter © 2002 Elsevier Science B.V. All rights reserved.
PII: S0301-4622(02)00292-2

virus particles from infected cells [4,5]. In both cases, however, the formation of the CsA/*h*Cyp18 complex is prerequisite for the CsA effects. Although great effort has been put in the investigation of this drug/*h*Cyp18 complex, published association constants show an enormous scattering from 1.6 nM to 5000 nM depending on the methods used [6–16]. It has been suggested that this wide spread might result from the combination of slightly different experimental conditions, large temperature coefficients and high sensitivity to solvent composition of the association reaction. In addition, the result often implies that the methods used to determine the association constant may not be adequate to assess tight-binding inhibitors. It has long been realized that the thermodynamics of the association reaction of CsA and cyclosporin derivatives with cyclophilins is vital to the analysis of biological CsA effects. Among the more than 40 gene-encoded cyclophilins *h*Cyp18 is the most abundant in human cells [17]. Assuming that the lower limit of published association constants readily describes the association process *h*Cyp18 would represent by the law of mass action the major CsA target in human cells. In contrast, a number of other cyclophilins would be relevant with respect to the upper limit of the association constants. Surprisingly, three-dimensional structures, determined by X-ray crystallography and nuclear magnetic resonance (NMR) spectroscopy gave a clear picture of complex composition and binding forces. Up to now, 18 structures of *h*Cyp18 complexed with CsA and its derivatives are reported in the Brookhaven Protein Data Bank (for review [12]). It results that the 1:1 stoichiometry is maintained throughout the structures by an active site directed attachment of CsA involving the side chain of the Trp^{121} residue of *h*Cyp18, 5 intermolecular hydrogen bonds between the drug and the protein, and a network of water-mediated contacts [18]. The $MeVal^{11}$ residue is particularly critical for CsA binding because of its positioning at the proline position of *h*Cyp18 substrates. One of the most pressing questions in the CsA field is how reliable parameters for the association reaction can be determined. In addition, knowledge of the whole set of thermodynamic factors that govern cyclophilin interactions with cyclosporin derivatives might lead to improved analyses of the huge number of distinct biological CsA effects observed until now [19].

We have taken an isothermal titration calorimetry approach to these issues. This method permits great flexibility in the choice of experimental conditions for monitoring the titration curves but has not yet been applied systematically to study the interaction of cyclophilins.

Association constants (K_a), binding enthalpies (ΔH) and changes in heat capacity (ΔC_p) of binding were determined as a function of pH, buffer composition, solvent viscosity and solvent deuterium isotope composition. The results confirm that ITC derived association constants closely match the magnitude of kinetically derived inhibition constants.

2. Experimental procedures

2.1. Materials

All chemicals and column resins were purchased from Merck and Sigma. D_2O was from ICN Biomedical Inc.

2.2. Protein expression and purification

A 6 l culture of *h*Cyp18 expressing *E. coli* strain M15 harboring the pQE70/*h*Cyp18 construct was grown in 2×YT medium supplemented with ampicillin (100 μg/ml) and kanamycin (50 μg/ml) at 37 °C to an A_{600} of 0.6. After inducing the expression of *h*Cyp18 with 1 mM IPTG, cells were incubated for 5 h at 37 °C. Cells were harvested by centrifugation at 4 °C for 15 min at 6000×*g* in a Beckmann J2-HC centrifuge; sedimented cells were resuspended and stored at −80 °C. Typically, 35 g of frozen cell paste was thawed and 2 volumes of cold buffer (20 mM tricine pH 8.0) were added. After homogenisation, cells were disrupted by passing them three times through a SLM Aminco french press® (Buettelborn, Germany) at 10 000 psi. After each passage, the lysed cell suspension was collected on ice. All subsequent steps were carried out at 4 °C. Cell debris and membrane parts were removed from the lysate by centrifugation for 1 h (100 000×*g* in a Beckman

L8 60 M ultracentrifuge). After the pH value of the supernatant had been adjusted to 8.0 the solution was applied to a Fractogel® EMD DEAE-650(M) (2.5×20 cm) anion exchange column equilibrated with 20 mM tricine buffer pH 8.0. The flowtrough was collected and applied to an affinity column Fractogel® TSK AF-Blue (1×6 cm). Human Cyp18 containing fractions were obtained by running a linear gradient from 0 to 3 M KCl in 200 ml of 20 mM tricine buffer pH 8.0. Enzymatically active fractions were collected and dialyzed two times against 2 l of 10 mM HEPES buffer pH 7.0. Subsequently, the sample was applied to a Fractogel® SO_3^- 650(M) exchange column, equilibrated with the same buffer. Using a 0–1 M NaCl gradient in 100 ml 10 mM HEPES pH 7.0 *h*Cyp18 was eluted from the column. From a typical preparation, 250 mg of *h*Cyp18 was obtained. The collected protein was better than 99% pure *h*Cyp18, as judged by SDS-PAGE and reversed phase HPLC. The same procedure was used to express and purify the *h*Cyp18F113A variant. Protein integrity was further confirmed by UV-CD spectroscopy, and the determination of the k_{cat}/K_m value related to the peptidyl prolyl *cis*/*trans* isomerase activity against the standard tetrapeptide substrate [20]. The active site concentration was determined exploiting the increase in fluorescence intensity of the Trp^{121} side chain upon CsA binding [6]. Compared to the spectroscopically determined enzyme concentration, using the calculated extinction coefficient of 8490 $M^{-1}\cdot cm^{-1}$ at 280 nm [21], 94% of the purified *h*Cyp18 binds to CsA.

2.3. Isothermal titration calorimetry

Isothermal titration calorimetry experiments were performed using a high precision VP-ITC titration calorimetric system (Microcal Inc. Northampton, MA). Samples of *h*Cyp18 were dialyzed exhaustively at 4 °C against the different buffers used for the titration experiments (see Section 3). Cyclosporin A stock solution was prepared in DMSO and dissolved in the same batch of buffer which was used for dialyzing *h*Cyp18. Final concentrations of CsA were 2–6 μM. Titration buffers had a maximum level of 0.5% (v/v) DMSO. The same amount of DMSO was added to the *h*Cyp18 sample used for titration to minimize the heat of dilution. All solutions were degassed under vacuum for 8 min with gentle stirring immediately before use. Because of the low solubility of CsA, it was used in the sample cell and titrated with *h*Cyp18 in the injection syringe. The protein concentration of *h*Cyp18 was determined shortly prior to measurement. The *h*Cyp18 concentration in the titration syringe was usually 10-fold higher than the CsA concentration used. To correct for heat effects not directly related to the binding reaction, control experiments were performed by making identical injections of the titrant into the sample cell containing buffer only. Control experiments were made at all temperatures used. The heat due to the binding reaction between the inhibitor and the enzyme was obtained as the difference between the heat of reaction and the heat of dilution. The titration curves were analyzed using Origin software provided with the instrument.

The same procedures were used for the experiments carried out in heavy water. Both *h*Cyp18 and CsA were allowed to exchange in D_2O at 20 °C for several hours before experiments were performed.

2.4. Spectroscopic methods

UV/VIS spectroscopic measurements were performed on a Hewlett Packard 8452 diode array UV/VIS spectrophotometer.

CD spectra were measured on a Jasco J-710 spectrometer. To measure the spectra in the near ultraviolet and the far ultraviolet region, cells of 10 and 1 mm optical path length were used, respectively. A single batch of 26 μM *h*Cyp18 solution in water was used for all experiments. To adjust the pH to the desired value in the range of pH 5 to 8 the protein solution was titrated with small volumes of diluted HCl and NaOH. Buffer spectra were numerically subtracted from protein spectra. The results were converted to residual ellipticities.

2.5. Thermodynamic parameter prediction method

Structure-based calculations were performed using an empirical parametrizations based on

changes in polar and apolar surface area [22,23]. The change in Accessible Surface Area (ΔASA) was calculated with the program Grasp [24]. The water probe used for calculation had a radius of 1.4 Å. Coordinates of the structure of *h*Cyp18 complexed with CsA were obtained from the Brookhaven Protein Data Bank (PDB file identifier: 1CWA). From these data, the changes in polar and apolar solvent-accessible surface area were calculated. The polar and apolar contributions to the total change in accessible surface were then used to calculate the change in heat capacity ΔC_p for the binding process, according to

$$\Delta C_{p\ calc} = a \cdot \Delta ASA_{nonpol} + b \cdot \Delta ASA_{pol} \quad (1)$$

Where a is 0.45 cal·K^{-1}·mol^{-1}·Å^{-2} and b is −0.26 cal·K^{-1}·mol^{-1}·Å^{-2} [22].

3. Results

3.1. Temperature dependence of CsA/hCyp18 interaction

A prerequisite for a precise calorimetric determination of the binding enthalpy is a good signal to noise ratio, and, therefore, high sample concentrations would be required. On the other hand, only low concentrations of the interacting partners can prevent a too steep transition of the titration curve if tightly binding inhibitors are being analyzed. Simultaneous determination of binding enthalpies and association constants require, therefore, the lowest possible concentration of reactants capable of producing a sufficient amount of heat to obtain a good signal to noise ratio. In our case, CsA solutions in the range from 2 to 6 μM resulted in a titration curve which allowed us to determine the binding enthalpy and the binding constant with high accuracy. A typical titration curve is given in Fig. 1. Multiple measurements of ΔH_{ITC} and K_a of the CsA/*h*Cyp18 interaction at 298 K using different concentrations and protein samples resulted in $\Delta H = -14.7 \pm 0.3$ kcal·mol^{-1} and a K_a of $(0.88 \pm 0.3) \cdot 10^{-8}$ M^{-1}. For all titrations, the calculated stoichiometry of binding was between 0.96 and 1.02, indicating a 1:1 binding stoichiometry. Control experiments performed by titrating a 50 μM CsA solution into 5 μM *h*Cyp18, resulted

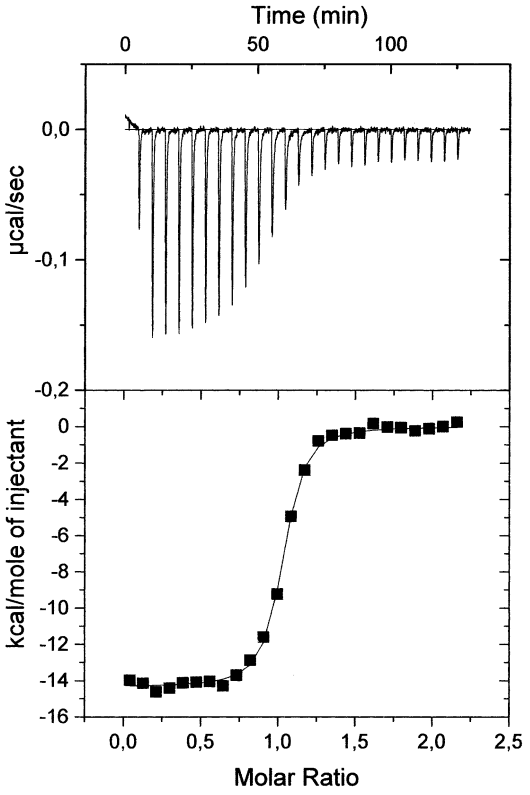

Fig. 1. Typical calorimetric titration of CsA binding to *h*Cyp18 at 25 °C in 25 mM phosphate buffer pH 7.5 containing 0.5% DMSO. Each peak (top panel) represents the injection of 4 μl of a 66 μM *h*Cyp18 solution into a solution of 2.2 μM CsA. The heats were determined by integration of the injection peaks and correction for mixing heats determined in a different experiment. The resulting titration curve (lower panel) was fitted to a single binding site model by non-linear least-squares analysis. The obtained thermodynamic parameters for this association process were as follows: $\Delta H = -1.431 \cdot 10^4 \pm 80$ kcal·mol^{-1} and $K_a = 9.292 \cdot 10^7 \pm 0.1 \cdot 10^7$ M, with a binding stoichiometry of 1.003 ± 0.005. The error of each parameter represents the error of fitting.

in the same binding stoichiometry (data not shown). To determine the change in heat capacity associated with the binding process, complete ITC experiments were performed at five different temperatures ranging from 278 to 306 K. The results are presented in Fig. 2 and summarized in Table 1. The binding reactions were carried out in 25 mM phosphate buffer at pH 7.5. Phosphate buffer was used because it is known to have only a small enthalpy of ionization ($\Delta H_{Ionization} = 1$ kcal·mol^{-1})

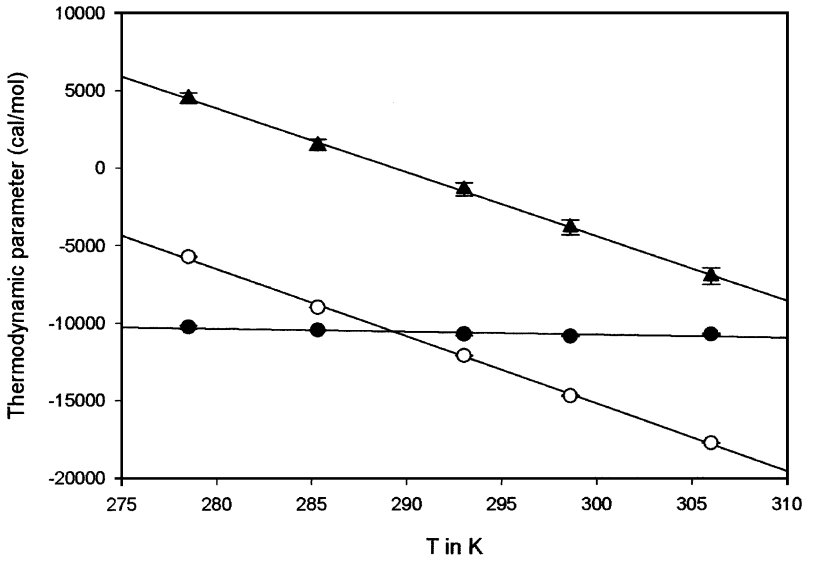

Fig. 2. Enthalpy (ΔH_{ITC}, open circles), entropy ($T\Delta S_{ITC}$, filled triangles) and free energy (ΔG^0, filled circles) from association of CsA with *h*Cyp18 as a function of temperature. All measurements were performed at pH 7.5 in 25 mM phosphate buffer containing 0.5% DMSO. Error bars are calculated from least square fit analysis of the heat of binding using the 1:1 binding model provided by the VP-ITC manufacturer. The drawn lines represent the linear regression of the data.

in conjunction with only a slight pK_a change with rising temperature ($\Delta pK_a/dT = -0.0028\ K^{-1}$). Therefore, the observed binding enthalpy ΔH_{ITC} was not corrected for possible protonation/deprotonation effects upon binding. ΔH_{ITC} and $T\Delta S_{ITC}$ strongly depend on temperature, while ΔG^0 is almost insensitive to the change of temperature as shown in Fig. 2. A plot of ΔH_{ITC} vs. temperature shows a linear relationship, and from the slope the change in heat capacity upon binding was $\Delta C_p = -435.8 \pm 7$ cal·mol^{-1}·K^{-1}. A plot of ΔH_{ITC} vs. $T\Delta S$ values for the binding of CsA at different temperatures shows a slope near unity (data not shown) that is common for binding processes like antibody/antigen recognition [25,26], protein/ligand interaction [27–30], and has been described as enthalpy/entropy compensation. Measured binding enthalpies over the examined temperature range are exothermic with $\Delta H_{ITC\ (25°C)} = -14.7 \pm 0.3$ kcal·mol^{-1}. Down to a temperature of 289 K the complex formation is entropically unfavourable and entirely driven by the exothermic binding enthalpy. Thermodynamic parameters for ligand-protein interaction can be related to changes in solvent accessible surface area upon binding. From the crystal structure we calculated the expected changes in heat capacity (using $\Delta ASA_{polar} = -357.3$ Å^2 and $\Delta ASA_{apolar} = -660.6$ Å^2) as described in Section 2. The calculated heat capacity change of the binding process according to Eq. (1) is significantly less negative ($\Delta C_{p\ calc} = -211$ cal·mol^{-1}·K^{-1}) than the experimentally determined change in heat capacity (Table 2).

3.2. pH dependence of the CsA/hCyp18 interaction

ITC experiments were performed twice at each pH value in the range from pH 5.0 to 8.2. For these experiments a triple buffer was used that allowed for constant buffering conditions and ionic strength throughout the investigated pH range [31]. The data derived from these calorimetric titrations are shown in Table 3. These data were fitted to a model of single proton linkage involving the change in pK_a of ionizable groups upon binding. Because CsA is devoid of ionizable groups it is

Table 1
Comparison of the temperature dependence of the thermodynamic parameters for the binding of CsA to *h*Cyp18 determined by isothermal titration calorimetry in buffers of different compositions. The error of each parameter represents the error of fitting

T (K)	ΔG^0 (kcal·mol^{-1})	$K_a \cdot 10^{-8}$ (M^{-1})	ΔH_{ITC} (kcal·mol^{-1})	$T\Delta S_{ITC}$ (kcal·mol^{-1})
25 mM phosphate buffer pH 7.5 in H_2O				
278.5	−10.3±0.1	1.1±0.3	−5.7±0.02	4.5
285.3	−10.5±0.05	1.0±0.2	−8.9±0.02	1.5
293.0	−10.7±0.1	0.97±0.1	−12.1±0.03	−1.4
298.0	−10.9±0.03	0.88±0.1	−14.7±0.03	−3.8
306.0	−10.7±0.06	0.46±0.04	−17.8±0.03	−7.0
25 mM phosphate buffer pH 7.5 in H_2O+30% glycerol				
280.7	−10.2±0.1	0.9±0.05	−11.6±0.03	−1.3
288.0	−10.6±0.1	1.2±0.1	−14.5±0.05	−3.8
293.2	−10.6±0.1	0.86±0.1	−16.0±0.06	−5.4
298.0	−10.5±0.2	0.61±0.06	−18.6±0.09	−7.8
303.0	−10.2±0.1	0.25±0.03	−21.2±0.2	−11.0
25 mM phosphate buffer pD 7.5 in D_2O				
280.7	−10.7±0.1	2.1±0.5	−6.2±0.04	4.5
283.5	−11.0±0.1	2.7±0.6	−7.7±0.04	3.3
287.9	−11.0±0.1	2.1±0.3	−9.6±0.04	1.4
293.2	−11.2±0.1	2.3±0.3	−11.6±0.04	−0.3
298.0	−11.1±0.2	1.5±0.5	−14.8±0.1	−3.6
303.0	−11.0±0.1	0.79±0.09	−17.1±0.08	−6.2

Table 2
Comparison of the experimentally determined data and structure-based calculations of the change in heat capacity upon CsA/*h*Cyp18 complex formation

ΔASA_{total}	-1017.9 Å^2
$\Delta ASA_{nonpolar}$	-660.6 Å^2
ΔASA_{polar}	-357.3 Å^2
$\Delta C_{p\ calc}$	-211 cal·mol^{-1}·K^{-1}
$\Delta C_{p\ measured}$	-435.8 ± 7 cal·mol^{-1}·K^{-1}

*h*Cyp18 where the pK_a change has to occur. Eq. (2) represents the model used for analyzing the experimental data, $(pK_a)_b$ and $(pK_a)_f$ refer to the pK_a value of *h*Cyp18 ionizable groups in the inhibitor bound and unbound state, K_a the association constant of the deprononated complex and K_{obs} represents the association constant measured in the ITC experiment. Best-fit parameters to this model are $K_a = 1.3 \cdot 10^8$ M^{-1}, $(pK_a)_f = 5.7$ and $(pK_a)_b < 4.5$. The pK_a value of an ionizable group involved in the binding process was determined to be 5.7 in the free state $(pK_a)_f$ and below 4.5 for the bound state $(pK_a)_b$. A precise determination of $(pK_a)_b$ was not possible because *h*Cyp18 tends to denature at low pH values.

$$K_{obs} = K_a \cdot \frac{1 + 10^{(pK_a)_b - pH}}{1 + 10^{(pK_a)_f - pH}} \quad (2)$$

Fig. 3 shows the plot of log K_{obs} vs. pH. The binding process shows a pH dependence similar to the data obtained by titration experiments detecting the enhancement of the tryptophan[121] fluorescence of *h*Cyp18 upon CsA binding [32]. In the acidic range, the association constant decreases approximately by factor nine from $1.4 \cdot 10^8$ M^{-1} to $1.6 \cdot 10^7$ M^{-1}. The measured ΔH_{ITC} values are not shown since interpretation in terms of proton linkage are difficult due to the different enthalpic contribution that arises from the exchange of protons with the various buffer components at different pH values. To rule out the possibility that pH-induced structural changes caused the observed pH dependence of the association constant, we measured near and far UV-CD spectra for *h*Cyp18 over the pH range which was used for the titration experiments. CD spectra do not change over the pH range from 5.0 to 8.0 (Fig. 4).

3.3. ΔH_{ITC} as a function of $\Delta H_{Ionization}$

The pH dependence of K_{obs} suggested that protons are transferred from the CsA/*h*Cyp18 complex to buffer ions at constant pH value. By using several single component buffers with different enthalpies of ionization ($\Delta H_{Ionization}$) one can determine the amount of protons transferred during the binding process using Eq. (3) [33].

$$\Delta H_{ITC} = \Delta H_{Binding} + n \cdot \Delta H_{Ionization} \quad (3)$$

where ΔH_{ITC} is the observed binding enthalpy during the experiment, $\Delta H_{Ionization}$ is the ionization enthalpy of buffer, $\Delta H_{Binding}$ is the buffer independent binding enthalpy, and n gives the net number of protons transferred during the binding process. It should be noted that n is positive when protons are transferred to the binding complex, and vice versa. Fig. 5 shows the observed binding enthalpy for the CsA/*h*Cyp18 formation measured in different buffers at pH 5.5 and pH 7.5 at 10 °C. The slopes of the solid lines indicate a release of one-half of a proton at pH 5.5 and virtually no proton transfer at pH 7.5.

4. Influence of viscous cosolvents and heavy water

The discrepancies between the measured and calculated heat capacity changes of the CsA/*h*Cyp18 interaction lead us to the assumption that water molecules might play an important role in the thermodynamics of this binding process. Such effects of ordered water molecules in the binding interface of protein/ligand complexes have been

Table 3
Thermodynamic binding parameter obtained from two independent measurements of CsA binding to *h*Cyp18 in triple buffer over the pH range from 5.0 to 8.2

PH	$K_a \cdot 10^{-8}$ (M^{-1})	
5.0	0.17	0.15
5.5	0.53	0.57
6.0	0.93	0.8
6.5	0.93	1.1
7.0	1.1	0.92
7.5	1.41	1.23
8.2	1.4	1.6

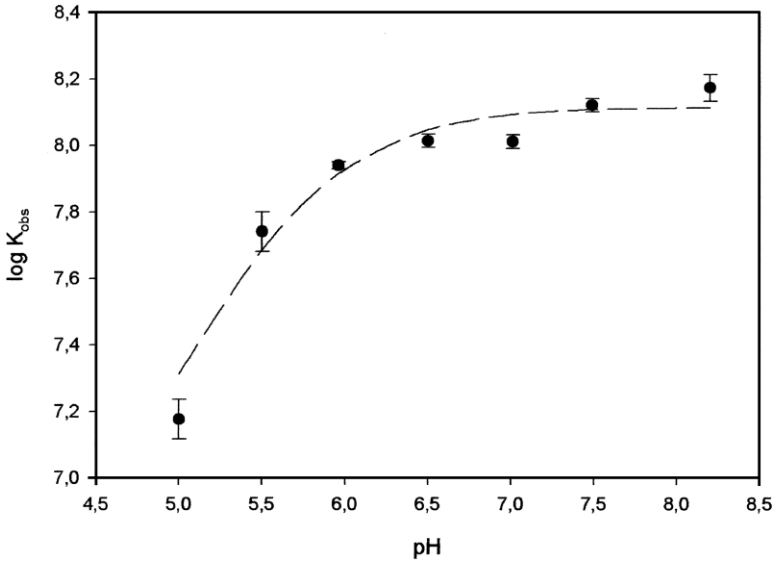

Fig. 3. pH dependence of the *h*Cyp18/CsA association constant (K_{obs}) measured in buffer containing 25 mM sodium acetate, 25 mM MES, 25 mM Tris, 150 mM sodium chloride and 0.5% DMSO. The dashed line is the best fit to a one proton linkage model [Eq. (2)] as described in the text.

described for other interactions as summarized from Holdgate et al. [34]. Solvent perturbation experiments are useful tools to investigate the role of water molecules in the binding interface of protein/ligand complexes [27,35,36]. To elucidate the influence of water on the thermodynamics of CsA/*h*Cyp18 complex formation, we performed isothermal titration calorimetry experiments in buffered solutions of H_2O (pH 7.5), D_2O (pD 7.5) and 30% (v/v) glycerol in the temperature range from 280 to 303 K. The results are summarized in Table 1. Fig. 6 shows the temperature dependence of the ΔH_{ITC} in D_2O and 30% (v/v) glycerol in comparison with the data obtained in H_2O. As one can see from the different slopes of the linear regression lines, the change in heat capacity of the binding reaction carried out in heavy water is significantly lower than in buffered H_2O solutions

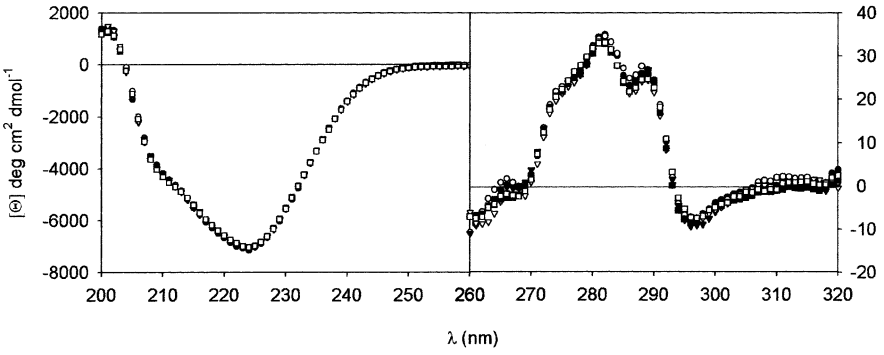

Fig. 4. CD-spectra of *h*Cyp18 at different pH values (from pH 5 to 8), recorded in the far and near UV range. 10 scans in the range of 200 to 260 nm and 260 to 320 nm were averaged for each pH value. The resulting spectra were normalized to molar ellipticities.

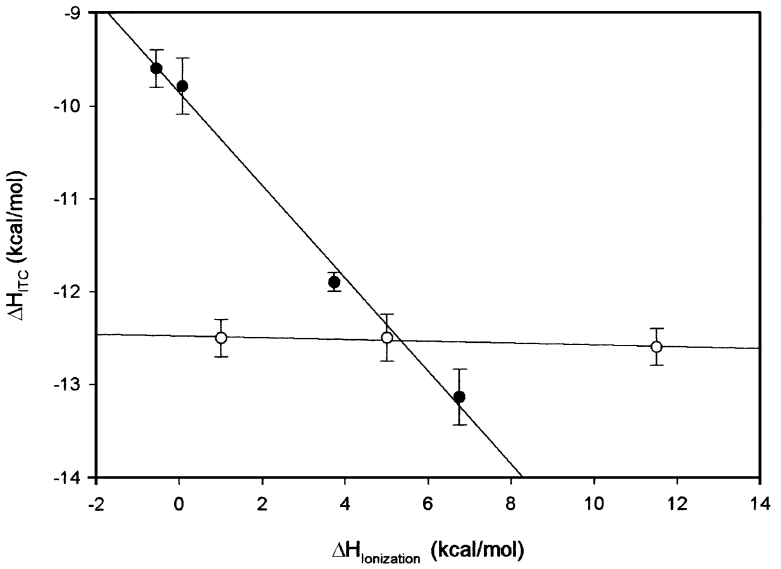

Fig. 5. Calorimetry-measured enthalpy as a function of buffer ionization enthalpy at pH 5.5 (closed circles) and 7.5 (open circles). Four different buffers over a wide range of ionization enthalpy were used (1, cacodylate buffer $\Delta H_{\text{Ionization}} = -0.56$ kcal·mol^{-1}; 2, acetate buffer $\Delta H_{\text{Ionization}} = 0.07$ kcal·mol^{-1}; 3, MES buffer $\Delta H_{\text{Ionization}} = 3.73$ kcal·mol^{-1} and 4, bistris buffer $\Delta H_{\text{Ionization}} = 6.75$ cal·mol^{-1}). According to Eq. (3), the slope of the linear regression yields the number of protons released by the buffer upon binding ($n = -0.5$ and $-8.6 \cdot 10^{-3}$ at pH 5.5 and at pH 7.5, respectively).

($\Delta\Delta C_{\text{p (H2O-D2O)}} = 52.3$ cal·mol^{-1}·K^{-1}). In contrast, the slope of the linear regression of the binding enthalpy (ΔH_{ITC}) in 30% (v/v) glycerol is almost the same as in water ($\Delta\Delta C_{\text{p (H2O-Glycerol)}} = -9.4$ cal·mol^{-1}·K^{-1}), yet, the binding enthalpy itself is significantly more negative in the glycerol solution ($\Delta\Delta H_{\text{ITC (H2O-Glycerol) (25 °C)}} = 3.9$ kcal·mol^{-1}). The decreased binding enthalpy does not lead to an increased association constant of the complex because of the compensating effect of the binding entropy ($T\Delta\Delta S_{\text{ITC (H2O-Glycerol) (25 °C)}} = 4$ kcal·mol^{-1}). The most striking result is that the binding constant increases in heavy water by more than a factor of two over the entire temperature range examined (Table 1). One must point out that the error for the determination of such high binding constants is relatively large, but even so the differences measured seem to be significant.

5. Discussion

We used isothermal titration calorimetry to determine thermodynamic parameters of the CsA/*h*Cyp18 complex formation over a wide range of experimental conditions. Neither temperature nor buffer composition gave rise to an extraordinary sensitivity of the magnitude of the association constant to experimental conditions. The value of $K_{\text{obs}} = 1.1 \cdot 10^8$ M^{-1} (at 10 °C as estimated from the regression line of ΔG in Fig. 2) changes just by factor two in the temperature range of 5 to 33 °C, and only minor changes occurred in the pH range from 6.5 to 8.2. The K_{obs} value of $(0.88 \pm 0.3) \cdot 10^8$ M^{-1} at 25 °C found in this study is considerably larger than the respective value of $0.2 \cdot 10^8$ M^{-1} found in HEPES/saline buffer [11]. Under all conditions, *h*Cyp18 binds CsA to a 1:1 stoichiometry ruling out the existence of additional low affinity binding sites as could be found for linear peptides [37].

Other methods used for determining binding constants of the CsA/*h*Cyp18 complex can be divided into four groups; (1) enzymatically derived inhibition constants K_i [6–10,38] (2) association constants measured by fluorescent CsA derivative displacement titrations [15] (3) associ-

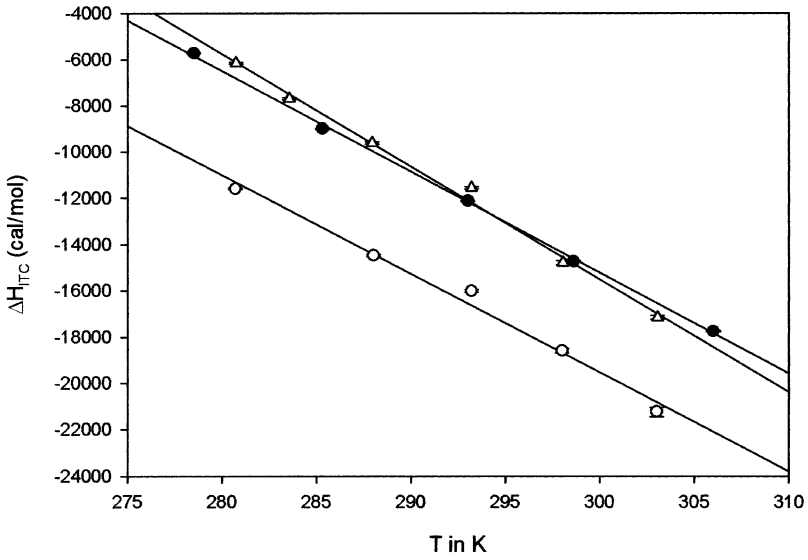

Fig. 6. Enthalpies of binding of CsA in H_2O (closed circles), D_2O (open triangles) and 30% glycerol (open circles) as a function of temperature. All solutions contained 25-mM phosphate buffer pH (pD) 7.5 and 0.5% DMSO. The solid lines represent the result of the linear regression of the experimental data. Error bars are calculated from least square fit analysis of the heat of binding using the 1:1 binding model provided by the VP-ITC manufacturer.

ation constants obtained from direct measurements, surface plasmon resonance techniques, *h*Cyp18 Trp^{121} fluorescence enhancement [9,11,14,16] and (4) ligand mobility shift Sephadex LH-20 column assay [13]. Comparing the binding constants estimated by different methods it is evident that the inhibition constants are much smaller (in the range of 1.6 to 17 nM) than the constants derived from tryptophan fluorescence enhancement titrations and surface plasmon resonance measurements ($K_{d\ app}$ from 30 to 205 nM). Such a dichotomy between inhibition and dissociation constant was observed earlier for the *bovine* cyclophilin18 (*b*Cyp18) and discussed as to arise from differences in the CsA binding site and the catalytic pocket of *b*Cyp18 [9]. It is unclear whether the methods are differently sensitive to the various aspects of the complex formation including oligomerization of the constituents of the association reaction [18,39,40]. Nevertheless, the ITC-derived association constants we report here correlate well with the lower limit of the inhibition constants reported, indicating that the kinetic approach to determine the affinity of CsA to *h*Cyp18 apparently reflects the true binding constant. The remaining difference between ITC-derived association constants and enzyme inhibition experiments might be attributed to differences in the experimental conditions like the high *h*Cyp18 concentrations used in the ITC approach (up to 100 μM; 100 000 fold higher than used in assays determining inhibition constants) that might couple the association reaction to protein oligomerization [40]. Additional support for the hypothesis that ITC experiments provide the true association constants was provided by the ITC analysis of the *h*Cyp18F113A variant. The reported K_i value of 190 nM [10] was even higher than the calculated K_d value of 85 nM (at 10 °C) determined by ITC (data not shown). Taken together, there is no evidence for a CsA binding site different from the catalytic pocket of *h*Cyp18.

Therefore, the cause of low affinity-related constants may also lie in the experimental procedures themselves. The thermodynamic survey of the highly specific CsA/*h*Cyp18 interaction presented shows that the complex formation is enthalpically driven with $\Delta H_{ITC} = -14.7 \pm 0.3$ kcal·mol^{-1} at 25 °C. The binding is associated with an unfavor-

able entropy of $T\Delta S_{ITC} = -3.8$ kcal·mol^{-1}. Fig. 2 shows the temperature dependence of all thermodynamic parameters for the CsA/*h*Cyp18 interaction. As described for many other protein/ligand interactions [25–30], we observed a strong linear temperature dependence of $T\Delta S_{ITC}$ and ΔH_{ITC}. As pointed out by Ha et al. [41] this is a direct consequence of a large ΔC_p value, since $(\partial\Delta H/\partial T)_p = \Delta C_p$ and $(\partial(T\Delta S)/\partial T)_p = \Delta C_p + \Delta S$, and then if $|\Delta C_p| \gg |\Delta S|$, the changes in ΔH and $T\Delta S$ with temperature will be roughly the same $(=\Delta C_p)$ and compensate each other. Therefore, ΔG itself is almost unaffected over the temperature range investigated. As described in Section 2 the measured temperature independent change in heat capacity (ΔC_p) can be correlated to the change of solvent exposed surface area. According to Eq. (1) a negative ΔC_p arises if non-polar solvent accessible surface area is reduced upon binding and hence indicates that hydrophobic interactions contribute to the CsA/*h*Cyp18 interaction. From this structure-based calculations $\Delta C_{p\ calc} = -211$ cal·mol^{-1}·K^{-1} resulted that is at variance with the experimentally determined value of -435.8 ± 7 cal·mol^{-1}·K^{-1}. Other authors describe a similar overestimation of ΔC_p using this relation [34,42–45]. One reason pointed out by these authors is that conformational changes of the reactants prior to binding lead to differences in solvent accessible surface area compared to the area calculated from the complex structure. In our case, the structure of the complexed and uncomplexed form of *h*Cyp18 has been solved [18,46]. Judging from the crystal structures, *h*Cyp18 seems to be a rather rigid protein. Due to the low solubility of CsA, no structure in aqueous solution is available. NMR-spectroscopic [47] and kinetic investigations [48] showed that multiple conformations of CsA exist and that tight binding to *h*Cyp18 occurs only if all CsA bonds are in *trans* conformation. In addition to the effects arising from the miscalculation of the solvent accessible surface area of different CsA conformations, Ladbury et al. [42] suggested that upon protein/ligand interaction dynamic fluctuations of the interfacial side-chains, solvent exposed backbone elements and their associated hydration sites are severely restricted and can thus lead to a more negative ΔC_p. As already mentioned, CsA binding does not seem to change the conformation of *h*Cyp18 in a very dramatic manner [49]. Interestingly, the NMR structure [50] revealed that two fragments of *h*Cyp18 (residues 68–72 and residues 101–104) reduce their flexibility upon CsA binding. Taken these conformational and protein dynamic effects together a more negative ΔC_p than calculated from the change in solvent accessible surface area seems reasonable. Holdgate et al. [34] proposed that these effects can be described quantitatively if one takes water molecules into consideration which are sequestered in the binding interface upon complex formation. They proposed that ΔC_p is lowered by approximately 48 ± 31 cal·mol^{-1}·K^{-1} for each trapped water molecule in the binding interface. Since the CsA/*h*Cyp18 interaction is mediated by five water molecules the corrected $\Delta C_{p\ calc}$ value is -451 ± 155 cal·mol^{-1}·K^{-1} which is in closer agreement with the experimentally obtained value. CsA is a very hydrophobic compound and the binding pocket of *h*Cyp18 is described as a hydrophobic crevice [18] one might, therefore, expect that the hydrophobic effect is the driving force responsible for the tight interaction. Contrarily, the reaction is entirely enthalpically driven and no favorable contributions to the free energy are made by the entropic term. Similar observations have been made by other authors [25,26,45,51] and were interpreted as both effects being important for the stability of the complex [52] or that because of the lack of an entropic contribution to the free energy of binding the role of the hydrophobic effect was neglected [45]. It can be argued that the increased order of sequestered water molecules lead to stiffer internal modes of vibration which generates a negative contribution not only to ΔC_p but also to $T\Delta S$. This could explain why $T\Delta S$ is unfavorable for the association of two hydrophobic interaction partners as in the CsA/*h*Cyp18 complex. To address the role of water in the binding interface in more detail we performed titration experiments in buffer solutions with reduced water activity and in heavy water.

The addition of 30% glycerol decreases the CsA/*h*Cyp18 complex stability by approximately -0.4 kcal·mol^{-1} ($\Delta\Delta G^0_{(H_2O\text{-Glycerol})(25\ ^\circ C)} = -0.4$ kcal·mol^{-1}). Glycerol was chosen because it does

not change the ionic strength and the macroscopic dielectric constant of the buffer solution [53]. High concentrations of glycerol have been reported to promote the destabilization of a complex if water is required in the binding interface. The decrease in free energy of binding is mainly due to the dramatic decrease in binding entropy $T\Delta\Delta S_{\mathrm{ITC}\ (\mathrm{H_2O\text{-}Glycerol})(25\ ^\circ\mathrm{C})} = 4$ kcal·mol^{-1}. Besides lowering the water activity in solution high glycerol concentrations also increase the viscosity of the solvent, this affects the entropic term of protein/ligand interactions. The most important contribution to the binding entropy arises from solvent reorganization, ΔS_{solv}, from the reduction in conformational degrees of freedom in the protein and the inhibitor, ΔS_{conf} and from the reduction in rotational/translational degrees of freedom, ΔS_{rt}:

$$\Delta S = \Delta S_{\mathrm{conf}} + \Delta S_{\mathrm{solv}} + \Delta S_{\mathrm{rt}}. \quad (4)$$

The solvent-related entropy is approximately equal to $\Delta C_{\mathrm{p}}\cdot\ln(T/385)$. The translational/rotational entropy for an 1:1 binding stoichiometry is approximately -8 cal K^{-1}·mol^{-1} [54]. Since ΔS_{solv} is only slightly affected by glycerol ($\Delta\Delta C_{\mathrm{p}\ (\mathrm{H_2O\text{-}Glycerol})} = -9.4$ cal·mol^{-1}·K^{-1}) and the reduction in rotational/translational degrees of freedom should not be changed, differences in ΔS are mainly due to a change arising from the reduced conformational degrees of freedom ($\Delta\Delta S_{\mathrm{conf}\ (\mathrm{H_2O\text{-}Glycerol})} = 11$ cal·K^{-1}·mol^{-1}). This is consistent with experimental evidence that glycerol increases the rigidity and the conformational heterogeneity of proteins as well as thermal backbone fluctuations [55–57]. The large decrease in binding entropy is partially compensated by a decrease in binding enthalpy $\Delta\Delta H_{\mathrm{ITC}\ (\mathrm{H_2O\text{-}Glycerol})(25\ ^\circ\mathrm{C})} = 3.9$ kcal·mol^{-1}. Using published transfer data [58] of model compounds from water to glycerol, Dürr et al. [35] calculated a mean enthalpy of transfer of hydrophobic side chains from water to glycerol as 0.96 ± 0.47 cal·mol^{-1}· Å^{-2} at 25 °C. Using this approximation and the calculated change in non-polar solvent accessible surface upon complex formation we can estimate a change in binding enthalpy of only 0.3–0.9 kcal·mol^{-1}. This is somewhat on the small side and obviously there must be other sources of the enthalpic stabilization induced by glycerol. Dürr et al. [35] argued that glycerol decreases the specific volume and the adiabatic compressibility of proteins and might, therefore, increase the favorable enthalpic interaction in folded proteins. The same effect can contribute to the binding enthalpy of the CsA/*h*Cyp18 interaction in glycerol. If water is a specific participant in the formation of the CsA/*h*Cyp18 complex, an increase in the apparent association constant should be observed in D_2O. The stronger binding should manifest itself in a more favorable binding enthalpy in D_2O [59]. Such an isotope effect was in fact observed. In heavy water, the free energy of binding is significantly more negative throughout the entire temperature range (Table 1) yielding association constants approximately two-fold of those in light water. Beside this direct effect, D_2O can also lead to tighter hydrogen bonds by substituting exchangeable protons in the protein and the inhibitor. Both effects might contribute to the quite large increase in binding affinity. The stronger interaction in D_2O at higher temperatures ($T > 297$ K) is due to the increased binding enthalpy, whereas at lower temperatures the higher binding entropy leads to stronger binding. As a thermodynamic parameter which connects ΔH and ΔS, the differences of the temperature independent heat capacity change in D_2O and H_2O are causing these effects ($\Delta\Delta C_{\mathrm{p}\ (\mathrm{H_2O\text{-}D_2O})} = 52.3$ cal·mol^{-1}·K^{-1}). Conelly et al. [60] described the thermodynamic analysis of the FK506/*h*FKBP12 and rapamycin/*h*FKBP12 association in heavy water. FKBP12 is the prototypic member of the FKBP subfamily of PPIases. They observed, in contrast to the CsA/*h*Cyp18 interaction, that the binding enthalpy in D_2O is less negative over the range of temperature examined. The change in heat capacity for the rapamycin/*h*FKBP12 interaction was less negative in D_2O and not changed in the FK506/*h*FKBP12 system. In contrast to our results, they attribute the change in binding enthalpy solely to the described negative transfer enthalpy of non-polar compounds from H_2O to D_2O. These transfer effects which also occur in the CsA/*h*Cyp18 interaction in our case seem to be overcompensated at higher temperatures by the favorable enthalpic contribution of stronger hydrogen bonds in D_2O. This indicates that the mode of interaction in CsA/*h*Cyp18 and

FK506/*h*FKBP12 is different. Kinetic investigations illuminating the enzymatic mechanism of accelerating the peptidylprolyl *cis*/*trans* isomerisation by *h*FKBP12 and *h*Cyp18 lead to the same conclusion (for review [61]). Our results show that water plays an important role in the tight interaction of CsA and *h*Cyp18. To fully understand the thermodynamics of the CsA/*h*Cyp18 complex formation it is necessary to take the contribution of water molecules in the binding interface into consideration.

Since protonation and deprotonation events in the binding interface upon binding have a considerable effect on ΔH_{ITC} and ΔS_{ITC} and can, therefore, lead to misinterpretation of the thermodynamic data, the binding energetics of CsA to *h*Cyp18 were characterized as a function of pH and buffer ionization enthalpy. Analyzing our data according to Eq. (2) we determined a $(pK_a)_f$ value for the unbound *h*Cyp18 of 5.7, the $(pK_a)_b$ value for the complex *h*Cyp18 could not be obtained due to decreased protein stability at low pH. The significant shift of the pK_a value from 5.7 to below 4.5 during CsA binding is possibly due to the increased hydrophobic character of the binding pocket. Fluorescence and NMR spectroscopic pH titration experiments support this interpretation [32,62]. Since the change in the pK_a value upon CsA binding must result in deprotonation of a side chain in the binding interface we performed ITC experiments at pH 5.5 and 7.5 in buffers with different ionization enthalpies (Fig. 5). The slope of the regression line is -0.5 at pH 5.5 and close to zero at pH 7.5 indicating that protons are released from the protein upon binding of CsA if the pH is close to the pK_a value we calculated. No proton release is observed at pH 7.5, ensuring that the side chain is fully deprotonated at this pH. There are two terms contributing to the enthalpy of binding ($\Delta H_{Binding}$), which are $\Delta H_{Protonation}$ and an enthalpic term that does not depend on the protonation event ($\Delta H'$) Eq. (5) [63].

$$\Delta H_{Binding} = \Delta H' + n \cdot \Delta H_{Protonation} \quad (5)$$

From Eq. (3) and Eq. (5),

$$\Delta H_{ITC} = \Delta H' + n \cdot (\Delta H_{Protonation} + \Delta H_{Ionization}) \quad (6)$$

At pH 7.5 no proton exchange is detectable; therefore, n in Eq. (3) and Eq. (5) becomes zero. Assuming that $\Delta H'$ does not change in the pH range we used, we may say that $\Delta H'$ has the same value a ΔH_{ITC} at pH 7.5. Using this and transforming Eq. (6) to:

$$\Delta H_{Protonation} = (\Delta H_{ITC\ (pH\ 5.5)} - \Delta H_{ITC\ (pH\ 7.5)})/n - \Delta H_{Ionization} \quad (7)$$

one can now estimate the net enthalpic contribution of deprotonation at pH 5.5. The deprotonation of a side chain in the CsA/*h*Cyp18 binding interface liberates approximately 4.3 kcal·mol^{-1}. ($\Delta H_{Protonation} = -4.3$ kcal·mol^{-1}). The heats of protonation for carboxyl, ε-amino, phenolic and imidazole groups in proteins are 0, -10.5, -10 and -6.6 kcal·mol^{-1}, respectively [64]. Since there is no tyrosine residue in the binding pocket of *h*Cyp18, the side chain deprotonated upon CsA binding at pH 5.5 is most likely a histidine. Histidine^{126} would be the best candidate, since it is localized in the binding pocket of *h*Cyp18 in a distance of approximately 3.3 Å to the MeVal^{11} side chain of CsA. NMR-spectroscopic pH-titration experiments of the CsA/*h*Cyp18 complex in solution showed that this side chain undergoes a shift in pK_a from 6.3 to below 4.5 during CsA binding [62]. From our experiments we cannot exclude that other ionizable side chain provide additional contributions to the observed pH dependency of the CsA binding. It seems that the protonation of histidine^{126} at low pH is mainly responsible for the decreased affinity of CsA to *h*Cyp18. Consistent with this assumption mutational analysis by Zydowsky et al. [10] of the Histidine^{126} side chain *h*Cyp18 variant showed a dramatically reduced enzymatic activity (less than 1%) and reduced CsA binding affinity.

Interestingly, the enzymatic parameters k_{cat} and k_{cat}/K_M for the *h*Cyp18 catalyzed *cis* to *trans* isomerisation of the model substrate Suc-Ala-Phe-Pro-Phe-pNA [65] show a comparable pH dependence as the association constant for CsA binding. The K_M value for an enzyme following a Michaelis–Menten kinetic includes the association constant for substrate binding (K_s) as well as the k_{cat} value, therefore, a decrease in k_{cat} results in a decrease in the association constant K_s. This indi-

cates that the association constant of the substrate molecule shows a similar pH dependence as the tight binding inhibitor CsA. The calculated pK_a for the pH dependence of k_{cat}/K_M value is 5.8, very close to the pK_a value we obtained for *h*Cyp18 in the free state, indicating that the same ionizable group might play an important role in CsA binding and in enzymatic catalysis.

Acknowledgments

The sequencing of the protein N-terminus by Dr P. Rücknagel and determination of the molecular mass by Dr A. Schierhorn is gratefully acknowledged. This work was supported by a grant from the Fonds der Chemischen Industrie.

References

[1] G. Fischer, B. Wittmann-Liebold, K. Lang, T. Kiefhaber, F.X. Schmid, Cyclophilin and peptidyl-prolyl *cis-trans* isomerase are probably identical proteins, Nature 337 (1989) 476–478.

[2] J. Liu, J.D.J.R. Farmer, W.S. Lane, J. Friedman, I. Weissman, S.L. Schreiber, Calcineurin is a common target of cyclophilin–cyclosporin A and FKBP-FK506 complexes, Cell 66 (1991) 807–815.

[3] J. Friedman, I. Weissman, Two cytoplasmic candidates for immunophilin action are revealed by affinity for a new cyclophilin—one in the presence and one in the absence of CsA, Cell 66 (1991) 799–806.

[4] S.R. Bartz, E. Hohenwalter, M.K. Hu, D.H. Rich, M. Malkovsky, Inhibition of human immunodeficiency virus replication by non-immunosuppressive analogs of cyclosporin A, Proc. Natl. Acad. Sci. USA. 92 (1995) 5381–5385.

[5] J. Luban, K.L. Bossolt, E.K. Franke, G.V. Kalpana, S.P. Goff, Human immunodeficiency virus type-1 gag protein binds to cyclophilin-A and cyclophilin-B, Cell 73 (1993) 1067–1078.

[6] J. Liu, M.W. Albers, C.M. Chen, S.L. Schreiber, C.T. Walsh, Cloning, expression, and purification of human cyclophilin in *Escherichia coli* and assessment of the catalytic role of cysteines by site-directed mutagenesis, Proc. Natl. Acad. Sci. USA 87 (1990) 2304–2308.

[7] M.J. Bossard, P.L. Koser, M. Brandt, D.J. Bergsma, M.A. Levy, A single Trp121 to Ala121 mutation in human cyclophilin alters cyclosporin A affinity and peptidyl–prolyl isomerase activity, Biochem. Biophys. Res. Commun. 176 (1991) 1142–1148.

[8] J.L. Kofron, P. Kuzmic, V. Kishore, G. Gemmecker, S.W. Fesik, D.H. Rich, Lithium chloride perturbation of *cis–trans* peptide bond equilibria—effect on conformational equilibria in cyclosporin-A and on time-dependent inhibition of cyclophilin, J. Am. Chem. Soc. 114 (1992) 2670–2675.

[9] P. Gallo, F. Rossi, M. Saviano, C. Pedone, G. Colonna, R. Ragone, Specific interaction between bovine cyclophilin a and synthetic analogues of cyclolinopeptide A, J. Biochem. 124 (1998) 880–885.

[10] L.D. Zydowsky, F.A. Etzkorn, H.Y. Chang, et al., Active site mutants of human cyclophilin-A separate peptidyl—prolyl isomerase activity from cyclosporin-A binding and calcineurin inhibition, Protein Sci. 1 (1992) 1092–1099.

[11] D. Seebach, H.G. Bossler, R. Flowers, E.M. Arnett, Calorimetric measurements of the complexation of cyclosporin A, ascomycin, fujimycin, and rapamycin with lithium chloride and with an immunophilin, Hel. Chim. Acta 77 (1994) 291–305.

[12] W. Braun, J. Kallen, V. Mikol, M.D. Walkinshaw, K. Wüthrich, Three-dimensional structure and actions of immunosuppressants and their immunophilins, FASEB J. 9 (1995) 63–72.

[13] R.E. Handschumacher, M.W. Harding, J. Rice, R.J. Drugge, D.W. Speicher, Cyclophilin: a specific cytosolic binding protein for cyclosporin A, Science 226 (1984) 544–547.

[14] M.W. Harding, R.E. Handschumacher, Cyclophilin, a primary molecular target for cyclosporine. Structural and functional implications, Transplantation 46 (2S) (1988) 29S–35S.

[15] P. Kuzmic, M.L. Moss, J.L. Kofron, D.H. Rich, Fluorescence displacement method for the determination of receptor-ligand binding constants, Anal. Biochem. 205 (1992) 65–69.

[16] G. Zeder-Lutz, M.H. Van Regenmortel, R. Wenger, D. Altschuh, Interaction of cyclosporin A and two cyclosporin analogs with cyclophilin: relationship between structure and binding, J. Chromatogr. B Biomed. Appl. 662 (1994) 301–306.

[17] G. Fischer, Peptidyl–prolyl cis/trans isomerases and their effectors, Angew Chem. Int. Edit. 33 (1994) 1415–1436.

[18] V. Mikol, J. Kallen, G. Pflugl, M.D. Walkinshaw, X-ray structure of a monomeric cyclophilin A-cyclosporin A crystal complex at 2.1 A resolution, J. Mol. Biol. 234 (1993) 1119–1130.

[19] G. Fischer, S. Grabley, R. Thiericke, Impact of natural products on cell biology: Low-molecular mass effectors of folding helper proteins, Drug Discovery from Nature PG. 257–280, 2000.

[20] G. Fischer, H. Bang, C. Mech, Nachweis einer Enzymkatalyse fur die *cis-trans*-Isomerisierung der Peptidbindung in prolinhaltigen Peptiden, Biomed. Biochim. Acta 43 (1984) 1101–1111.

[21] S.C. Gill, P.H. von Hippel, Calculation of protein extinction coefficients from amino acid sequence data, Analyt. Biochem. 182 (1989) 319–326.

[22] K.P. Murphy, E. Freire, Thermodynamics of structural stability and cooperative folding behavior in proteins, Adv. Protein Chem. 43 (1992) 313–361.
[23] D. Xie, E. Freire, Structure based prediction of protein folding intermediates, J. Mol. Biol. 242 (1994) 62–80.
[24] A. Nicholls, K.A. Sharp, B. Honig, Protein folding and association: insights from the interfacial and thermodynamic properties of hydrocarbons, Proteins 11 (1991) 281–296.
[25] K.A. Hibbits, D.S. Gill, R.C. Willson, Isothermal titration calorimetric study of the association of hen egg lysozyme and the anti-lysozyme antibody HyHEL-5, Biochemistry (Mosc) 33 (1994) 3584–3590.
[26] C.P. Swaminathan, A. Nandi, S.S. Visweswariah, A. Surolia, Thermodynamic analyses reveal role of water release in epitope recognition by a monoclonal antibody against the human guanylyl cyclase C receptor, J. Biol. Chem. 274 (1999) 31272–31278.
[27] T.K. Dam, S. Oscarson, C.F. Brewer, Thermodynamics of binding of the core trimannoside of asparagine-linked carbohydrates and deoxy analogs to *Dioclea grandiflora* lectin, J. Biol. Chem. 273 (1998) 32812–32817.
[28] L. Cervoni, I. Lascu, Y. Xu, P. Gonin, M. Morr, M. Merouani, J. Janin, A. Giartosio, Binding of nucleotides to nucleoside diphosphate kinase: a calorimetric study, Biochemistry 40 (2001) 4583–4589.
[29] K. Bachhawat-Sikder, C.J. Thomas, A. Surolia, Thermodynamic analysis of the binding of galactose and poly-*N*-acetyllactosamine derivatives to human galectin-3, FEBS Lett. 500 (2001) 75–79.
[30] M.C. Chervenak, E.J. Toone, Calorimetric analysis of the binding of lectins with overlapping carbohydrate-binding ligand specificities, Biochemistry 34 (1995) 5685–5695.
[31] K.J. Ellis, J.F. Morrison, Buffers of constant ionic strength for studying pH-dependent processes, Methods Enzymol. 87 (1982) 405–426.
[32] M. Gastmans, G. Volckaert, Y. Engelborghs, Tryptophan microstate reshuffling upon the binding of cyclosporin A to human cyclophilin A, Proteins 35 (1999) 464–474.
[33] B.M. Baker, K.P. Murphy, Evaluation of linked protonation effects in protein binding reactions using isothermal titration calorimetry, Biophys. J. 71 (1996) 2049–2055.
[34] G.A. Holdgate, A. Tunnicliffe, W.H. Ward, et al., The entropic penalty of ordered water accounts for weaker binding of the antibiotic novobiocin to a resistant mutant of DNA gyrase: a thermodynamic and crystallographic study, Biochemistry 36 (1997) 9663–9673.
[35] E. Durr, I. Jelesarov, Thermodynamic analysis of cavity creating mutations in an engineered leucine zipper and energetics of glycerol-induced coiled coil stabilization, Biochemistry 39 (2000) 4472–4482.
[36] Y. Shi, S. Wang, S. Krueger, F.P. Schwarz, Effect of mutations at the monomer–monomer interface of cAMP receptor protein on specific DNA binding, J. Biol. Chem. 274 (1999) 6946–6956.
[37] L. Demange, M. Moutiez, K. Vaudry, C. Dugave, Interaction of human cyclophilin hCyp-18 with short peptides suggests the existence of two functionally independent subsites, FEBS Lett. 505 (2001) 191–195.
[38] B. Janowski, G. Fischer, Modulation of cyclosporin A/cyclophilin interactions by drug vehicles, Bioorg. Med. Chem. 5 (1997) 179–186.
[39] R.B. Knott, M. Capel, S. Hansen, R.E. Handschumacher, A small-angle X-ray scattering study of the binding of cyclosporin A to cyclophilin, J. Appl. Crystallogr. 28 (1995) 546–552.
[40] G. Pflugl, J. Kallen, T. Schirmer, J.N. Jansonius, M.G. Zurini, M.D. Walkinshaw, X-ray structure of a decameric cyclophilin–cyclosporin crystal complex, Nature 361 (1993) 91–94.
[41] J.H. Ha, R.S. Spolar, M.T. Record, Role of the hydrophobic effect in stability of site-specific protein-DNA complexes, J. Mol. Biol. 209 (1989) 801–816.
[42] J.E. Ladbury, J.G. Wright, J.M. Sturtevant, P.B. Sigler, A thermodynamic study of the trp repressor-operator interaction, J. Mol. Biol. 238 (1994) 669–681.
[43] N.J. Faergeman, B.W. Sigurskjold, B.B. Kragelund, K.V. Andersen, J. Knudsen, Thermodynamics of ligand binding to acyl-coenzyme A binding protein studied by titration calorimetry, Biochemistry (Mosc) 35 (1996) 14118–14126.
[44] A.K. Samland, I. Jelesarov, R. Kuhn, N. Amrhein, P. Macheroux, Thermodynamic characterization of ligand-induced conformational changes in UDP-N-acetylglucosamine enolpyruvyl transferase, Biochemistry (Mosc) 40 (2001) 9950–9956.
[45] F.P. Schwarz, D. Tello, F.A. Goldbaum, R.A. Mariuzza, R.J. Poljak, Thermodynamics of antigen–antibody binding using specific anti-lysozyme antibodies, Eur. J. Biochem. 228 (1995) 388–394.
[46] H. Ke, L.D. Zydowsky, J. Liu, C.T. Walsh, Crystal structure of recombinant human T-cell cyclophilin A at 2.5 A resolution, Proc. Natl. Acad. Sci. USA 88 (1991) 9483–9487.
[47] P.F. Augustijns, S.C. Brown, D.H. Willard, et al., Hydration changes implicated in the remarkable temperature-dependent membrane permeation of cyclosporin A, Biochemistry (Mosc) 39 (2000) 7621–7630.
[48] J.L. Kofron, P. Kuzmic, V. Kishore, E. Colon Bonilla, D.H. Rich, Determination of kinetic constants for peptidyl prolyl *cis-trans* isomerases by an improved spectrophotometric assay, Biochemistry (Mosc) 30 (1991) 6127–6134.
[49] J. Kallen, V. Mikol, P. Taylor, M.D. Walkinshaw, X-ray structures and analysis of 11 cyclosporin derivatives complexed with cyclophilin A, J. Mol. Biol. 283 (1998) 435–449.
[50] M. Ottiger, O. Zerbe, P. Guntert, K. Wuthrich, The NMR solution conformation of unligated human cyclophilin A, J. Mol. Biol. 272 (1997) 64–81.

[51] P.L. Wintrode, P.L. Privalov, Energetics of target peptide recognition by calmodulin: a calorimetric study, J. Mol. Biol. 266 (1997) 1050–1062.
[52] D. Xu, S.L. Lin, R. Nussinov, Protein binding versus protein folding: the role of hydrophilic bridges in protein associations, J. Mol. Biol. 265 (1997) 68–84.
[53] M.J. Kornblatt, J.A. Kornblatt, G. Hui Bon Hoa, The role of water in the dissociation of enolase, a dimeric enzyme, Arch Biochem. Biophys. 306 (1993) 495–500.
[54] K.P. Murphy, D. Xie, K.C. Garcia, L.M. Amzel, E. Freire, Structural energetics of peptide recognition: angiotensin II/antibody binding, Proteins 15 (1993) 113–120.
[55] A.R. Bizzarri, S. Cannistraro, Solvent modulation of the structural heterogeneity in FeIII myoglobin samples: a low temperature EPR investigation, Eur. Biophys. J. 22 (1993) 259–267.
[56] B.D. Schlyer, D.G. Steel, A. Gafni, Long time-scale probing of the protein globular core using hydrogen-exchange and room temperature phosphorescence, Biochem. Biophys. Res. Commun. 223 (1996) 670–674.
[57] S.L. Butler, J.J. Falke, Effects of protein stabilizing agents on thermal backbone motions: a disulfide trapping study, Biochemistry (Mosc) 35 (1996) 10595–10600.
[58] K. Gekko, Enthalpy and entropy of transfer of amino acids and diglycine from water to aqueous polyol solutions, J. Biochem. (Tokyo) 90 (1981) 1643–1652.
[59] K.B. Schowen, R.L. Schowen, Solvent isotope effects of enzyme systems, Methods Enzymol. 87 (1982) 551–606.
[60] P.R. Connelly, J.A. Thomson, M.J. Fitzgibbon, F.J. Bruzzese, Probing hydration contributions to the thermodynamics of ligand binding by proteins-enthalpy and heat capacity changes of tacrolimus and rapamycin binding to FK506 binding protein in D_2O and H_2O, Biochemistry (Mosc) 32 (1993) 5583–5590.
[61] R.L. Stein, Mechanism of enzymic and non-enzymic prolyl cis/trans isomerization, Adv. Protein Chem. 44 (1993) 1–24.
[62] L. Yu, S.W. Fesik, pH titration of the histidine residues of cyclophilin and FK506 binding protein in the absence and presence of immunosuppressant ligands, Biochim. Biophys. Acta 1209 (1994) 24–32.
[63] I. Jelesarov, H.R. Bosshard, Thermodynamics of ferredoxin binding to ferredoxin:NADP+ reductase and the role of water at the complex interface, Biochemistry 33 (1994) 13321–13328.
[64] D.D. Shiao, J.M. Sturtevant, Heats of binding protons to globular proteins, Biopolymers 15 (1976) 1201–1211.
[65] M. Schutkowski, S. Wollner, G. Fischer, Inhibition of peptidyl–prolyl *cis/trans* isomerase activity by substrate analog structures: Thioxo tetrapeptide-4- nitroanilides, Biochemistry 34 (1995) 13016–13026.